Polaronic metal in lightly doped high-T_c cuprates

A. S. Mishchenko,[1,2] N. Nagaosa,[1,3] K. M. Shen,[4]
Z.-X. Shen,[5] X. J. Zhou,[6] and T. P. Devereaux[5]

[1]*Cross-Correlated Materials Research Group, RIKEN, 2-1 Hirosawa, Wako, Saitama, 351-0198, Japan*
[2]*RRC "Kurchatov Institute", 123182, Moscow, Russia*
[3]*Department of Applied Physics, The University of Tokyo, 7-3-1 Hongo, Bunkyo-ku, Tokyo 113, Japan*
[4]*Laboratory of Atomic and Solid State Physics, Department of Physics, Cornell University, Ithaca NY 14853, USA*
[5]*Department of Physics, Applied Physics, and Stanford Institute for Materials and Energy Sciences, SLAC National Accelerator Laboratory, Menlo Park, CA 94025 and Stanford University, Stanford, CA 94305 USA*
[6]*National Lab for Superconductivity, Institute of Physics, Chinese Academy of Sciences, Beijing 100190, China*

We present a combined study of the angle-resolved-photoemission spectroscopy (ARPES) and quantum Monte Carlo simulations to propose a novel polaronic metallic state in underdoped cuprates. An approximation scheme is proposed to represent underdoped cuprates away from 1/2 filling, replacing the many-body Hamiltonian by that of a single polaron with effective electron-phonon interaction (EPI), that successfully explains many puzzles such as a large momentum-dependent dichotomy between nodal and anti-nodal directions, and an unconventional doping dependence of ARPES in the underdoped region.

PACS numbers: 71.10.Fd,71.38.-k,02.70.Ss

It is established that the physics of high temperature superconductors is that of hole doping a Mott insulator [1, 2] where even a single hole is substantially influenced by many-body effects [3]. Understanding of the dynamics of holes in Mott insulators has attracted a great deal of interest [1, 3, 4]. The major interactions are electron-electron interactions (EEI) and EPI. The importance of the former is no doubt essential since the Mott insulator is driven by this EEI, while the latter was considered to be largely irrelevant to superconductivity based on the observations of a small isotope effect on the optimal T_c [5] and an absence of a phonon contribution to the resistivity [6].

On the other hand, there is now accumulating evidence that the EPI plays an important role in the physics of cuprates [7, 8]. In particular, EPI manifests itself in (i) an isotope effect on superfluid density ρ_s and T_c away from optimal doping [9], and (ii) neutron and Raman scattering [10–12] experiments showing strong phonon softening with both temperature and hole doping, indicating that EPI is strong [13]. Furthermore, the recent advancement in the energy/momentum resolution [14] of ARPES resulted in the discovery of the dispersion "kinks" at around 40-70meV measured from the Fermi energy, in the range of the relevant oxygen related phonons [15–17]. These particular phonons - oxygen buckling and half-breathing modes are known to soften with doping [10, 18] and with temperature [10–12, 16–18] and there is mounting evidence relating the kink to the phonon anomaly of the bond stretching phonons [19, 20]. The

quick change of the velocity can be predicted by any interaction of a quasiparticle with a bosonic mode, either with a phonon because of EPI [16, 17, 20, 21] or with a collective magnetic resonance mode [22, 23]. Early studies of the doping dependence of the kink revealed a "universality" of the kink energy for $La_{2-x}Sr_xCuO_4$ (LSCO) over the entire doping range [24] and casted doubts on the validity of the latter scenario as the energy scale of the magnetic excitation changes strongly with doping. More recent studies showed that there is a subtle doping dependence of the kink energy [25] which, nevertheless, can be explained within the framework of EPI scenario as well [21].

As a more direct test distinguishing between these two scenarios, an observation of an isotope effect just in the vicinity of the kink [26] and its explanation in terms of EPI [27] has given an additional argument in favor of a phononic origin of the kink. Furthermore, it was shown that the kink is observed in electron-doped cuprates around 40-70meV, i.e. at the same energies as the hole-doped ones [28]. Hence, it is clear that the kink is due to EPI with phonon modes, which are roughly at the same energies in hole- and electron-doped cuprates, and not because of coupling to a magnetic mode whose energy in the electron-doped compounds is not larger than 10 meV [29, 30].

Generally, there are two possible pictures of the EPI. One is the *Migdal-Eliashberg picture* where the kinetic (Fermi) energy of the electrons ε_F is much larger than the phonon energy Ω. In this limit, the multi-phonon processes represented by the vertex correction are suppressed by the Fermi degeneracy and reduced by the adiabatic factor Ω/ε_F, i.e., EPI is basically in the weak coupling region[31, 32]. The other limit is the *polaron picture* where ε_F is much smaller than Ω where the multi-phonon processes can, in principle, lead to the small polaron formation. The latter picture of the strong coupling limit of a polaron in *undoped* materials, where ARPES corresponds to the single hole dynamics in a Mott insulator, has been established by a detailed comparison between experiment [33–35] and theory [36–39]. The picture obtained there is that the "quasi-particle" peak observed experimentally is that of Franck-Condon multiphonon band, which follows the energy dispersion of bare t-J model without EPI, while the zero-phonon line has only a very small weight $Z << 1$. Namely the hole polaron is in the strong coupling small polaronic state.

At very *small dopings* it is clear that the Fermi energy ε_F of a few holes doped into the Mott insulator is smaller than the relevant phonon energy Ω. Then the polaronic energy dispersion can be inverted and the ARPES dispersion is cut-off by the (small) Fermi energy ε_F (measured from the hole side). In this case the adiabatic factor Ω/ε_F is not small and one cannot rely on the weak coupling Migdal-Eliashberg approach and, hence, has to treat the EPI in the polaron limit including all vertex corrections and without considerable approximations. The polaron paradigm is complementary to the conventional Migdal-Eliashberg picture for metals [31, 32], the latter of which fails to explain various anomalous features in the underdoped region. Therefore it is reasonable to apply the polaron picture in the underdoped region.

In the present paper we interpret the kink in underdoped cuprates as a result of a short-range Holstein-like interaction of a hole with optical phonons. Since the polaron scenario is more appropriate in the underdoped region than the Migdal-Eliashberg one, we approximate the interacting many-body Hamiltonian by the single hole polaronic Hamiltonian with an effective dimensionless coupling constant λ of EPI. The effective coupling constant λ in the weakly doped compound is renormalized in comparison with the bare constant λ_0, corresponding to the case of a single hole, by EEI. It is known for gas of Fröhlich polarons both theoretically and experimentally [40–44] that the basic properties of polarons behave with increasing concentration as if the coupling constant of the EPI is effectively reduced. Comparison with experiment shows that effects of weak EPI and Coulomb repulsion can be factorized in 2D systems in the light doping limit and, besides, this factorization is approximately valid up to a doping level $\delta \approx 0.1$ [40, 41]. Since the radius of Holstein polarons is smaller than that of Fröhlich ones we expect in our case better applicability of the modeling of the influence of doping by changing the effective EPI constant λ.

The above assumption indicates that λ should be regarded as the effective coupling constant in the trial Hamiltonian which best mimics the experimental results. Such an approach has been already applied to the explanation of the doping dependence of the optical absorption spectra of underdoped cuprates and it was shown that the effective coupling constant λ decreases with increasing doping [45].

Using the approximation-free Diagrammatic Monte Carlo (DMC) method [36, 46–49] we have calculated the momentum dependence of the Lehman spectral functions of a single hole in the extended $t-J$ model, i.e., $t-t'-t''-J-ph$ model (Fig. 1). Within this model a single hole in an antiferromagnet can hop up to the 3rd nearest neighbor ($t(1) \equiv t$, $t(2) \equiv t'$, and $t(3) \equiv t''$):

$$\hat{H}_{\mathrm{tt't''\text{-}J}} = -\sum_{n=1}^{3}\sum_{\langle ij,n\rangle\sigma} t(n) c^{\dagger}_{i\sigma} c_{j\sigma}$$

$$+ J\sum_{\langle ij\rangle}\left(\mathbf{S}_i\mathbf{S}_j - n_i n_j/4\right). \qquad (1)$$

Here $c_{j\sigma}$ is a projected (to avoid double occupancy) fermion annihilation operator, $n_i = \sum_\sigma c^{\dagger}_{i\sigma} c_{i\sigma} < 2$ is the occupation number, $\mathbf{S}_i$ is spin-1/2 operator, $\langle ij,n\rangle$ denotes neighboring sites on n-th coordination sphere

(circle) in a two-dimensional lattice. We note, that although long-range antiferromagnetic (AFM) order and AFM gap is destroyed at rather low doping levels, overdamped spin waves and short range AFM correlations, showing the largest interplay with short-range EPI, persist up to fairly high doping [50, 51]. Hence, the most important part of the interpaly between short-range AFM and short-range EPI survives at moderate dopings.

The hole also interacts with dispersionless optical phonons Ω via a short range Holstein coupling γ [52, 53]

$$\hat{H}^{\rm EPI} = \Omega \sum_{\mathbf{k}} b^{\dagger}_{\mathbf{k}} b_{\mathbf{k}}$$

$$+ N^{-1/2} \gamma \sum_{\mathbf{k},\mathbf{q}} \left[h^{\dagger}_{\mathbf{k}} h_{\mathbf{k}-\mathbf{q}} b_{\mathbf{q}} + h.c. \right] . \qquad (2)$$

(Here $b_{\mathbf{k}}$ and $h_{\mathbf{k}}$ are phonon and hole annihilation operators, respectively.) We define the dimensionless coupling constant $\lambda = \gamma^2/4t\Omega$ of the EPI. Our calculations are done for parameters which are required to reproduce the observed dispersions [34, 54] in $Sr_2CuO_2Cl_2$ (SCOC) [$J = 0.4t$, $t' = -0.34t$, $t'' = 0.23t$] and $\Omega = 0.2t$. The energies of the kink are 50-80 meV [15] and those of active phonons are 40-70 meV. Hence, with typical hopping amplitude $t \approx 0.4eV$ one finds $0.12 \leq \Omega/t \leq 0.2$. In further calculations we use spin-wave representation [55] and take into account only phonon-phonon vertex corrections. It was proved that the above approximations are reliable for the above parameters [55, 56].

The polaron picture for the finite doped case explains the dichotomy between nodal and antinodal points [57, 58]. The fact that the lifetime of the lowest peak in ARPES is large at the nodal point and small for the antinodal one, is a consequence of the contrasting nature of quasi-particle broadening by EPI at different energies and momenta in the intermediate and weak coupling regimes. If the energy of the hole at momentum $\mathbf{k}$, measured from the ground state of the Mott insulator in the nodal point is smaller than the phonon frequency Ω, the decay of the quasiparticle by phonon emission is forbidden by energy conservation law leading to the sharp peak. On the other hand, when the energy is larger than the phonon frequency (antinodal points, as an example) the real decay processes by phonon emission are allowed, causing significant line broadening even at moderate EPI coupling constants. For example, as it is seen from the calculated momentum dependence of the Lehman function (Fig. 1a,b), the linewidth abruptly increases when the quasi-particle dispersion crosses the phonon energy at $[k-\pi/2]/\pi \approx 0.17$. We emphasize that the interaction of holes with phonons is essential for the explanation of experimentally found "dichotomy". Although a broadening at general momentum $\mathbf{k}$ is present even in pure $tt't''-J$ model, it is considerably smaller than the experimental one and, more important, does not show a sharp threshold-like increase above $\sim 50-70$meV. Of course one can not rule out inhomogeneous source of broadening of antinodal quasiparticles (see, e.g. [59]) though the phonon mechanism is one of possible candidates to explain the "dichotomy".

The low-energy dispersion (close to Fermi level ε_F), where quasiparticles are sharp, is separated from the high-energy part by a kink, where the velocity of the quasiparticle abruptly changes [15, 24, 60]. Experiments show that the high-energy velocity above the bosonic mode Ω exhibits a strong doping dependence, while the doping dependence of the low-energy velocity is weaker [24]. Fig. 2a shows the experimentally extracted dispersions from LSCO [24]. These data were obtained using the momentum distribution curve (MDC) method, giving the so-called universal low-energy velocity behavior where the velocity below the kink energy is found to be largely insensitive to doping. In the framework of the MDC analysis one traces the momentum dependence of intensity at a fixed energy. Then, the point of maximal intensity is considered to be an energy-momentum point representing the dispersion of the quasiparticle.

DMC method is capable of obtaining the energy distribution curves (EDC) when one traces the energy dependence of the intensity keeping the momentum fixed. The reason is that the theoretical spectra here are obtained as analytic continuation to the real frequencies of imaginary time Green functions calculated by the DMC method at fixed momenta. Green functions calculated at different momenta possess slightly different distributions of statistical errorbars over the imaginary time. This difference is considerably amplified by the very high sensitivity of analytic continuation method to the distribution of statistical errors. Hence, in contrast to EDC method the MDC method is not reliable in the framework of the theoretical methodology used here.

In order to compare directly experimental results with the calculated EDC dispersion, we also re-analyze the low energy data using the traditional EDC method. The extracted MDC and EDC dispersions are plotted in Fig. 2a and the corresponding low- and high-energy velocities are summarized in Fig. 2b. The MDC and EDC dispersion curves are very similar in the weak coupling limit, except for energies which are very close to phonon frequency [7]. However, MDC and EDC curves in the strongly interacting systems, as it was already observed before for bi-layer manganite [61], are very different. The difference is especially large at low energies while the high energy data are rather insensitive to the type of analysis.

According to the analysis of the optical absorption [45], the EPI is enhanced with underdoping. Then, as is expected in the Migdal-Eliashberg picture, the velocity at low energy should get smaller with underdoping while the high energy "bare" velocity above the phonon frequency should not change. The observed behavior is different. In the framework of the experimental MDC

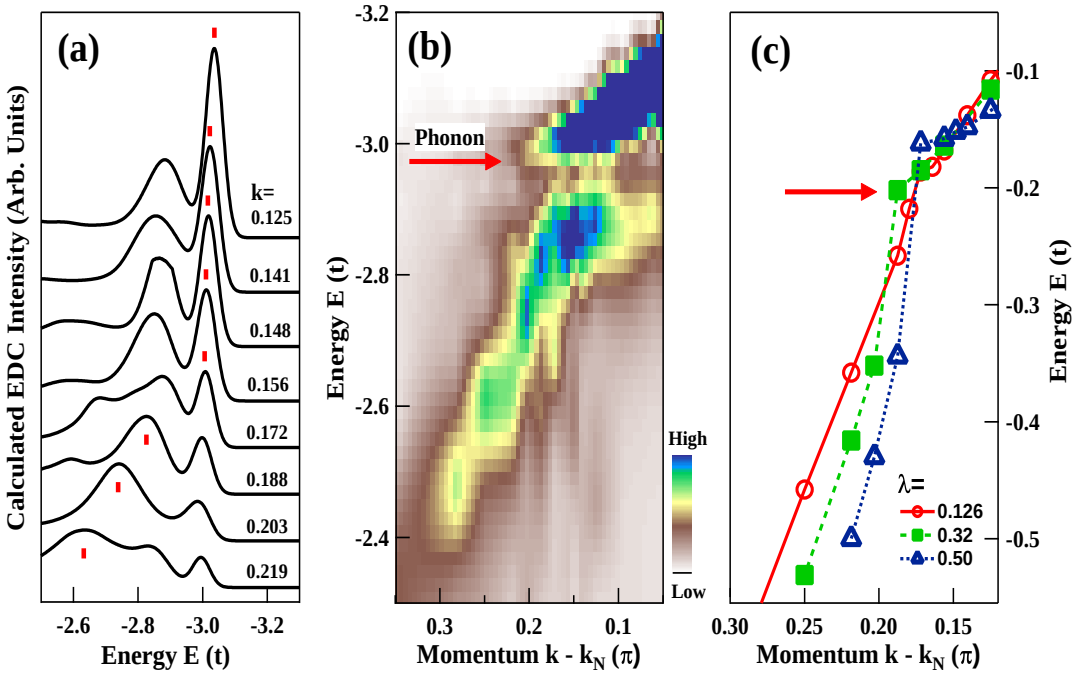

FIG. 1: (a) Evolution of the Lehman function along the nodal $(\pi/2, \pi/2) \rightarrow (0, 0)$ direction for $\lambda = 0.5$. Thick red lines indicate maxima of the Lehman function obtained from EDC analysis. (b) Intensity plot for the same parameters. Energy in panels (a-b) is counted from the vacuum state of the Hamiltonian (1-2). (c) Momentum dependence of the peaks in the Lehman function for $\lambda = 0.126$ (circles), $\lambda = 0.32$ (squares), and $\lambda = 0.50$ (triangles). Energy in panel (c) is counted from the top of polaron band at $\mathbf{k}_N = (\pi/2, \pi/2)$. The red arrow in (b) and (c) indicates the position of the phonon measured from the top of the polaron band. All energies are in the units of $t = 0.4$eV.

analysis (Fig. 2b), similar to the theoretical EDC results (Fig. 1c), the high-energy velocity *increases* with decreasing doping (Fig. 2b). While understanding the differences between EDC and MDC is a matter to be further explored, we compared EDC experimental result with EDC theoretical data which are only ones available from calculations done by DMC method.

In contrast to the Migdal-Eliashberg picture, a polaron picture in the intermediate coupling regime can give a consistent explanation of these unique features. We calculated ARPES spectra for different values of λ along the $(0, 0)$ - (π, π) nodal direction (Fig. 1c). Indeed, the energy of the ground state $E(\pi/2, \pi/2)$ of the Hamiltonians (1-2) depends on the coupling constant λ (Fig. 1a,b) and, thus, the energies of the kinks at different λs do not match to each other in the theoretical calculations. The energy onset in experiment is set in a different way. In the experimental data, presented in Ref. [24], the binding energy is counted from the Fermi energy ε_F and the origin of momentum is set to the Fermi momentum k_F where the quasi-particle dispersion crosses the Fermi energy. In this manner the energy of the kink in experimental data is roughly the same for all dopings [24]. Hence, to compare the results of our theoretical calculations with the experimental data for each λ in Fig. 1(c) we applied a constant energy shift to the theoretical results in order to match the energies of the quasi-particle for momenta just at the kink position. It is clear that the theoretical high-energy $V_{high}^{EDC}(\lambda)$ and low-energy $V_{low}^{EDC}(\lambda)$ velocities estimated just above and below the kink position, respectively, do not depend on the theoretical energy onset. However, both the high- and low-energy EDC velocities are dependent on coupling constant λ, representing the intrinsic quasiparticle behavior.

The calculated high-energy velocity (Fig. 1c) in terms of the polaron picture gives a qualitative explanation of the anomalous doping dependence of the high-energy velocity observed in LSCO provided one assumes that the effective coupling constant λ increases with underdoping. Indeed, one can see that, in contrast to the Migdal-Eliashberg picture, the theoretical high energy velocity $V_{high}^{EDC}(\lambda)$ (Fig. 1c) just above the kink position increases

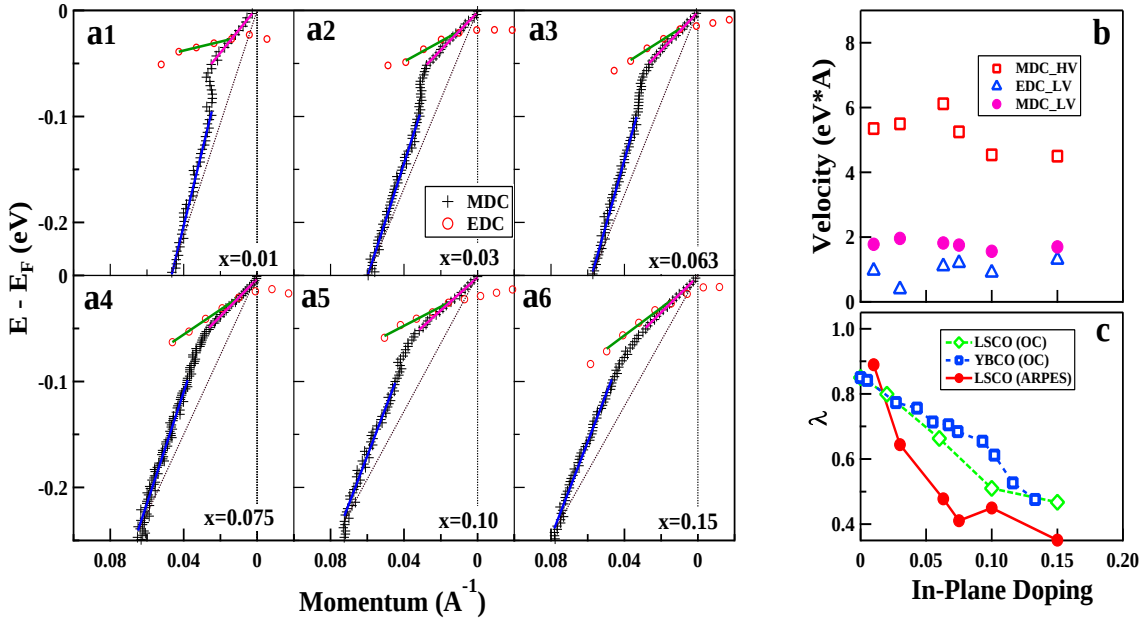

FIG. 2: (a). Energy-momentum dispersions for LSCO with different dopings, using both EDC and MDC methods. The MDC low (high) energy velocity V_{low} (V_{high}) is obtained by fitting MDC dispersion at binding energy 0∼50meV (100∼250meV) using a linear line. (b). Low and high-energy velocities as a function of doping obtained from MDC and EDC dispersions. (c). The EPI coupling constant obtained from EDC low-energy velocity and high energy velocity by empirical scaling relation (3) $\lambda = \sqrt{(V_{high}^{EDC}(\lambda) - V_{low}^{EDC}(\lambda))/V_{low}^{EDC}(\lambda)}/\sqrt{20}$ (filled circles). Empty squares and diamonds are coupling constants $\lambda^{(\mathrm{OC})}$ obtained from the analysis of the optical conductivity [45] on weakly doped LSCO and $YBa_2Cu_3O_{6+x}$ (YBCO), respectively. Only the ratio of $\lambda^{(\mathrm{OC})}(x)$ at finite doping x and of that $\lambda^{(\mathrm{OC})}(x=0)$ at zero doping is determined in Ref. [45] and we take $\lambda^{(\mathrm{OC})}(x=0) = 0.85$ to match results obtained from optical and ARPES measurements as close as possible.

with λ. Hence, according to experiment, the theoretical high energy velocity $V_{high}^{EDC}(\lambda)$ increases with underdoping.

Furthermore, from our theoretical results of the spectral function of a single hole in the $tt't'' - J - ph$ model (1-2), we can fit the dependence of the ratio $(V_{high}^{EDC}(\lambda) - V_{low}^{EDC}(\lambda))/V_{low}^{EDC}(\lambda)$ on the effective coupling constant λ by a quadratic empirical scaling relation:

$$\frac{(V_{high}^{EDC}(\lambda) - V_{low}^{EDC}(\lambda))}{V_{low}^{EDC}(\lambda)} \approx 20\lambda^2 \,. \qquad (3)$$

The doping dependence of the effective EPI constant λ of LSCO estimated from the comparison of the above theoretical relation with experimental data is shown in Fig. 2c. Note, that the values of λ obtained from ARPES are consistent with data derived from the doping dependence of the optical absorption [45] and other methods which take into account the strong interplay between EEI and EPI [7, 8]. We checked that the basic characteristics of the kink are mostly defined not by the range of EPI but by the resonance between the energy of the phonon and quasiparticle. Therefore, the data in Fig. 2c are also valid for the Fröhlich type of coupling. We note that our parameters are always in the large-polaron regime because EPI is less than the critical coupling $\lambda_c = 0.6$ for given model [62]. The restriction of our analysis to a single phonon mode does not influence the relation (3) because fine features, caused by interaction with multiple modes, do not change the gross shape of the kink [63].

Note here that the obtained effective λs are reasonably of the order or less than unity even in the strongly underdoped regime where it is maximal. This is in sharp contrast to the naive application of the Migdal-Eliashberg relation $(V_{high} - V_{low})/V_{low} = \lambda$ which would give an unphysically large number on the order of ~ 10 at low

dopings. It is clear that the Migdal-Eliashberg approach underestimates the effects of EPI because the vertex corrections are neglected which, in turn, leads to an overestimated value of the effective λ. Indeed, even generalized Migdal-Eliashberg approach, including electron-electron correlation effects [64, 65], predicts that $\lambda \approx 1.2$ in the optimal doping, which is 3 times larger than our result obtained with full vertex corrections included.

The values of λ at low dopings, obtained in this paper from the kink angle, coincide with that obtained from the linewidth and distance of Franck-Condon peak from the chemical potential in undoped La_2CuO_4 compound [38]. According to Fig. 1f in [15], the kink angle is a rather universal function and, hence, the performed analysis applies also to $La_{2-y-x}Nd_ySr_xCO_4$, $Bi_2Sr_2CuO_6$ and $Bi_2Sr_2CaCu_2O_8$.

In the vicinity of the kink (Fig. 1a) high resolution Lehman spectral functions consist of the ground state peak and several phonon sidebands. The origin of the kink is the abrupt transfer of spectral weight from the low energy peak to the phonon sidebands when the momentum is increased (Fig. 1a). The rate of transfer with momentum increase strongly depends on the EPI coupling constant and, thus, the velocity just above the kink energy is very sensitive to the EPI.

Note, that the high energy velocity V_{high} is more sensitive to EPI change than the renormalized low energy velocity V_{low} (Fig. 1c). We note that the domain of the fast high energy velocity $V_{\rm high}$ is restricted to an energy range of a few phonon frequencies Ω and to a small fraction of the Brillouin zone. Then, according to our calculations, at higher momenta/energies dispersion of the hump returns to the position of quasi-particle band noninteracting with phonons. The return of the quasi-particle dispersion to the unrenormalized one is typical also for the weak coupling theory and for the Migdal-Eliashberg approach neglecting the vertex corrections. However, in the intermediate coupling regime the energy/momentum domain of large velocity in exact DMC method is considerably wider than that obtained in a weak coupling approach.

Several phonon sidebands survive above the momentum of kink (Fig. 1a) though they are not seen (Fig. 1b) if the spectrum is broadened more than it follows from the Hamiltonian (1-2). Indeed there are numerous sources of decay, such as coming from hole-hole interaction, impurities, surface roughness etc., which do not enter the Hamiltonian (1-2). The intensity map where numerical data are broadened by Gaussian with the width $\sigma = 0.1$ does not show multiple sidebands but a single peak (Fig. 1b), which roughly corresponds to the energy of the highest intensity sideband. Comparing Figs. 1 and 2, the global features of the spectrum are well reproduced by our polaron picture, which provides an alternative and complementary approximation replacing Migdal-Eliashberg approach in the underdoped regime. Strictly speaking, general features of the evolution of the Lehmann spectral function across the phonon energy are not restricted to the $tt't'' - J - ph$ model since similar phenomena should be observed for any polaronic model with intermediate strength of EPI [66]. What is novel here is that a similar scenario is realized in a more complicated situation with a combination of Mott physics and EPI.

In conclusion, we propose a novel polaronic metal picture for underdoped cuprates and analyze the ARPES on underdoped cuprates in the framework of the polaronic scenario based on t-J model plus EPI. It is particularly important that the electron-lattice polaron is formed in the background of the antiferromagnetic correlations and the essential influence of the electron-phonon interaction on the spectra is observed exclusively due to constructive interplay between electron-lattice and electron-electron interaction. Indeed, strong effects of coupling of holes to the lattice vibrations are observed only because the latter are highlighted by concomitant interaction of holes with short-range antiferromagnetic correlations. The latter ones persist up to moderate dopings even when the long-range antiferromagnetic order is destroyed. The doped holes form the small polaron in the undoped and heavily underdoped region. Analysis of ARPES in this scenario shows that, in accordance with the results previously obtained from the analysis of optical absorption, effective EPI decreases gradually and reaches the self-trapping crossover at optimal doping. The extended (large polaron) and localized (small polaron) states coexist around this crossover region, which appear in a momentum dependent way. This picture explains many experimental puzzles, through the realistic estimate of the coupling constant, such as the large momentum-dependent broadening of a single hole spectral function, the dichotomy of nodal and anti-nodal direction, and the unconventional doping dependence of ARPES of underdoped cuprates.

We thank G. Sawatzky, O Gunnarsson, O. Rösch, G. Khaliullin, D. Tessa's, A. V. Chubukov, V. Cataudella, G. De Filippis, and C. Varma for valuable discussions. ASM is supported by RFBR grant 10-02-00047a. NN is supported by MEXT Grand-in-Aid No.20740167, 19048008, 19048015, and 21244053, Strategic International Cooperative Program (Joint Research Type) from Japan Science and Technology Agency, and by the Japan Society for the Promotion of Science (JSPS) through its "Funding Program for World-Leading Innovative R & D on Science and Technology (FIRST Program)". KMS acknowledges the National Science Foundation (DMR-0847385) and the Air Force Office of Scientific Research (Award No. FA9550-11-1-0033). TPD and ZXS are supported by the US Department of Energy, Office of Basic Energy Sciences under contract No. DE-AC02-76SF00515.

[1] Dagotto E., Rev. Mod. Phys. **66** (1994) 763.
[2] Lee P. A., Nagaosa N., and Wen X. G., Rev. Mod. Phys. **78** (2006) 17.
[3] Kane C. L., Lee P. A., and N. Read, Phys. Rev. B **39** (1989) 6880.
[4] Manousakis E., Rev. Mod. Phys. **63** (1991) 1.
[5] Batlogg B. et al, Phys. Rev. Lett. **58** (1987) 2333.
[6] Gunnarsson O., Calandra M., and Han J. E., Rev. Mod. Phys. **75** (2003) 1085.
[7] Gunnarsson O., and Rösch O., J. Phys.: Condens. Matter **20** (2008) 043201.
[8] Mishchenko A. S., Phys. Usp. **52** (2009) 1193.
[9] Khasanov R. et al, Phys. Rev. Lett. **92** (2004) 057602.
[10] L. Pintschovius L. and Braden M., Phys. Rev. B **60** (1999) R15039.
[11] Thomsen C. et al, Phys. Rev. B **37** (1988) 9860.
[12] Hadjiev V. G. et al, Phys. Rev. B **58** (1998) 1043.
[13] Khaliullin G. and Horsch P., Physica C **282-287** (1997) 1751.
[14] Damascelli A., Shen Z.-X., and Hussain Z., Rev. Mod. Phys. **75** (2003) 473.
[15] Lanzara A. et al, Nature **412** (2001) 510.
[16] Cuk T. et al, Phys. Rev. Lett. **93** (2004) 117003.
[17] Devereaux T. P. et al, Phys. Rev. Lett. **93** (2004) 117004.
[18] McQueeney R. J. et al, Phys. Rev. Lett. **82** (1999) 628.
[19] Graf J. et al, Phys. Rev. Lett. **100** (2008) 227002.
[20] De Filippis G. et al, Europhys. Lett. **91** (2010) 47007.
[21] Bauer J. and Sangiovanni G., Phys. Rev. B **82** (2010) 184535.
[22] Chubukov A. V. and Norman M. R., Phys. Rev. B **70** (2004) 174505.
[23] Eschrig M. and Norman M. R., Phys. Rev. Lett. **85** (2000) 3261; Phys. Rev. B **67** (2003) 144503.
[24] Zhou X. J et al, Nature **423** (2003) 398.
[25] Kordyuk A. A. et al, Phys. Rev. Lett. **97** (2006) 017002.
[26] Iwasawa H. et al, Phys. Rev. Lett. **101** (2008) 157005.
[27] Koikegami S. and Aiura Y., Phys. Rev. B **77** 2008 184519.
[28] Park S. R et al, Phys. Rev. Lett. **101** (2008) 117006.
[29] Wilson S. D. et al, Nature (London) **442** (2006) 59.
[30] Zhao J. et al, Phys. Rev. Lett. **99** (2007) 017001.
[31] Migdal A. B., Sov. Phys. JETP **7** (1958) 996.
[32] Mahan G. D., *Many Particle Physics* (Plenum Press, New york, 1990).
[33] Shen K. M. et al, Phys. Rev. Lett. **93** (2004) 267002.
[34] Wells B. O. et al, Phys. Rev. Lett. **74** (1995) 964.
[35] Shen K. et al, Phys. Rev. B **75** (2007) 075115.
[36] Mishchenko A. S. and Nagaosa N., Phys. Rev. Lett. **93** (2004) 036402.
[37] Rösch O. and Gunnarsson O., Eur. Phys. J. B **43** (2005) 11.
[38] Rösch O. et al, Phys. Rev. Lett. **95** (2005) 227002.
[39] Cataudella V. et al, Phys. Rev. Lett. **99** (2007) 226402.
[40] Tempere J. and Devreese J. T., Phys. Rev. B **64** (2001) 104504.
[41] Tempere J. and Devreese J. T., Eur. Phys. J. B **20** (2001) 27.
[42] van Mechelen J. L. M. et al, Phys. Rev. Lett **100** (2008) 226403.
[43] Devreese J. T. et al, Phys. Rev. B **81** (2010) 125119.
[44] Meevasana V. et al, New J. Phys. **12** (2010) 023004.
[45] Mishchenko A. S. et al, Phys. Rev. Lett. **100** (2008) 166401.
[46] Prokof'ev N. V. and Svisitunov B. V., Phys. Rev. Lett. **81** (1998) 2514.
[47] Mishchenko A. S. et al, Phys. Rev. B **62** (2000) 6317.
[48] Mishchenko A. S., Phys. Usp. **48** (2005) 887.
[49] Mishchenko A. S. and Nagaosa N., J. Phys. Soc. Japan **75** (2006) 011003.
[50] Carvalho Dias F. and Pimentel I. R., Phys. Rev. B **71** (2005) 224412.
[51] Kastner M. A. et al, Rev. Mod. Phys. **70** (1998) 897.
[52] Rösch O. and Gunnarsson O., Phys. Rev. Lett. **92** (2004) 146403.
[53] Ishihara S. and Nagaosa N., Phys. Rev. B **69** (2004) 144520.
[54] Xiang T. and Wheatley M., Phys. Rev. B **54** (1996) R12653.
[55] Liu Z. and Manousakis E., Phys. Rev. B **45** (1992) 2425.
[56] Gunnarsson O. and Rösch O., Phys. Rev. B **73** (2006) 174521.
[57] Zhou X. J. et al, Phys. Rev. Lett. **92** (2004) 187001.
[58] Shen Z.-X. and Schrieffer J. R., Phys. Rev. Lett. **78** (1997) 1771.
[59] Alldredge J. M. et al, Nature Phys. **4** (2008) 319.
[60] Bogdanov P. V. et al, Phys. Rev. Lett. **85** (2000) 2581.
[61] Norman M. R. et al, Phys. Rev. B **64** (2001) 184508.
[62] Mishchenko A. S. and Nagaosa N., Phys. Rev. B **73** (2006) 092502.
[63] Zhou X. J. et al, Phys. Rev. Lett. **95** (2005) 117001.
[64] Mazur E. A., Europhys. Lett. **90** (2010) 47005.
[65] Johnston S. et al, Phys. Rev. B **82** (2010) 064513.
[66] Hohenadler M., Aichhorn M. and von den Linden W., Phys. Rev. B **68** (2003) 184304.